2007 IEEE International Conference on
Robotics and Automation
Roma, Italy, 10-14 April 2007

Development of a Master Slave System with Force Sensing Using Pneumatic Servo System for Laparoscopic Surgery

Kodak Tadano
Interdisciplinary Graduate School of Science and Engineering
Tokyo Institute of Technology
Email: tadano@k-k.pi.titech.ac.jp

Kenji Kawashima
Precision and Intelligence Laboratories
Tokyo Institute of Technology
Email: kkawashi@pi.titech.ac.jp

Abstract— **In the teleoperated minimally invasive surgery systems, measurement and display of sense of force to the operator is a problem. In this paper, a manipulator for supporting forceps has been developed which has 3-DOFs actuated by pneumatic cylinders. We also developed a master manipulator using a delta mechanism and a gimbal mechanism with a force sensor and motors with reduction gears. In the developed master-slave system, we applied different impedance control to each manipulator. The force control type of impedance control is adopted without force sensor for the pneumatic slave manipulator. For the master manipulator the motion control type of impedance control is implemented. The experimental results indicated that the operator could feel the force at the slave side to a satisfactory extent.**

I. Introduction

Minimally invasive laparoscopic surgery is an effective method as alternative to open surgery. However, it requires increased skill on the part of the surgeon. This is because the degrees of freedom (DOFs) of surgical instruments in laparoscopic surgery are restricted due to trocars. To solve the above problems, robotic manipulators, which have multi-DOFs at their tip, have been reported as alternative to conventional instruments [1][2][3][4].

In order to realize safer and more precise operation using robotic manipulator especially master-slave system, force measurement and feedback are very important [5][6]. To realize a precise position control of the manipulator, using electric motors with high reduction gears is effective while the effect of gravity, inertia and friction have small influence on the actuator. Sensing the accurate force with such manipulators need a force sensor at near the tip. However, the sensor at the end of forceps manipulator makes sterilizing and downsizing difficult. On the other hand, the direct drive motors or little reduced motors, with high back drivability, enable estimation of the external force without using force sensors[7][8]. These motors with sufficient power are too large and heavy to use for compact robots. Moreover, when pulling the plug causes, the manipulator could not keep the condition.

We have developed a 4-DOFs forceps manipulator which is able to estimate external force without force sensors using pneumatic cylinders[9]. Pneumatic actuators have higher mass-power ratio and can generate larger force without reduction mechanism. Also, the manipulator could keep the condition with having flexibility by shutting the valve even when pulling the plug caused.

In this paper, we newly developed a pneumatic manipulator supporting the forceps for a surgical master-slave system. The prototype manipulator has 3-DOFs which are driven by pneumatic cylinders. We also developed a master manipulator which have delta mechanism and serial gimbal mechanism. Then, a bilateral control using impedance control is applied to the master-slave system.

This paper is organized as follows. In section II, we describe the mechanism of the newly developed manipulator. In section III, the developed master manipulator is shown. Then, in section IV, the proposed bilateral control method is introduced. Experimental results of the system performance are shown in section V, and concluding remarks are given in section VI.

II. Developed manipulator to support the forceps

Fig. 1 shows the developed manipulator. The manipulator has 3-DOFs that consists of 2 rotational DOFs on a trocar point and a translational DOF. This manipulator premises that the forceps manipulator mounted on it has the rotational DOF on the forceps axis. Combining two parallel link

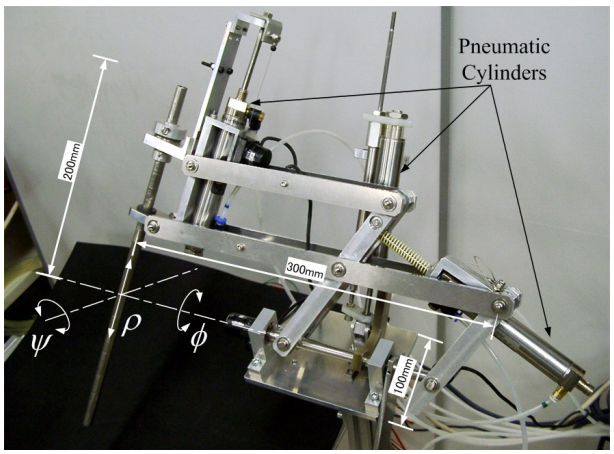

Fig. 1. Developed manipulator

TABLE I
WORKING RANGE AND MAXIMUM FORCE/TORQUE

	ϕ	ψ	ρ
working range	$\pm$ 52 deg	$\pm$ 50 deg	$\pm$ 37.5 mm
force/torque	3.7 Nm	6.0 Nm	132 N

mechanism and gimbal mechanism, the point of trocar is immovable mechanically without direct support. Therefore, the load to the patient's body can be minimized and the kinematics calculation does not need the coordinate of the port position. The gravity effect is compensated mechanically using counter weight.

Single rod type pneumatic cylinders (Airpel,M16D75U, diameter : 15.9mm, rod diameter : 5.0mm , stroke : 75mm) were used for driving the each joint. This cylinder uses a precision fit graphite piston which slides freely - without lubrication - inside a pyrex glass cylinder. Therefore, their own friction is negligible small.

At the joint of ϕ axis, the linear motion of the cylinder is transformed to the rotation using a slider-rocker mechanism as shown Fig. 2. Then, the relationship between the displacement of the piston X and the rotation angle ϕ is given by

$$X = d\tan\phi \tag{1}$$

where d denotes the length as shown in Fig. 2. Therefore, the torque τ_ϕ at this axis can be obtained from the force of the cylinder F_ϕ by the principle of virtual work as follows

$$\tau_\phi = \frac{\partial X}{\partial \phi} F_\phi \tag{2}$$

$$= d(1+\tan^2\phi)\, F_\phi \tag{3}$$

At the joint of ψ axis, we adopted a slider-crank mechanism as shown Fig. 3. The torque of the joint is also represented as follows:

$$L = \sqrt{r^2 + h^2 + 2rh\sin\psi'} \tag{4}$$

$$\tau_\psi = \frac{\partial L}{\partial \psi} F_\psi \tag{5}$$

$$= \frac{rh\cos\psi'}{\sqrt{r^2+h^2+2rh\sin\psi'}}\, F_\psi \tag{6}$$

$$\psi' = \psi + \psi_0 \tag{7}$$

where L, r, h are lengths as shown in Fig. 3. Table I shows the motion ranges and maximum forces of each joint when the supply pressure is 800kPa(abs). The power of the manipulator can be limited easily and reliably by reducing the supply pressure.

Fig. 4 shows the system configuration of the manipulator. The pressure sensors are installed at the valve side of the air tubes. The pressure drop and the delay are confirmed to be small. If we replace the encoders by optical fiber type, the manipulator could be separated from electrical components completely. Then, it becomes not only easy to sterilize but available under MRI environment using nonmagnetic materials.

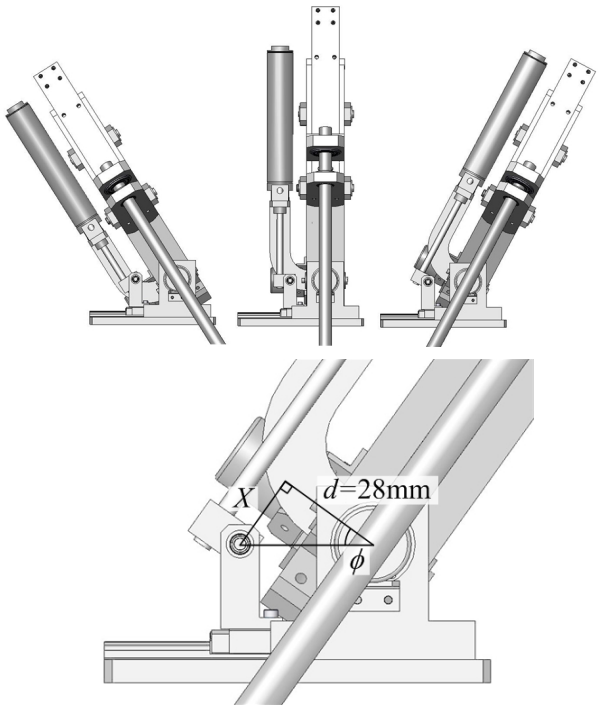

Fig. 2. Slider-Rocker Mechanism

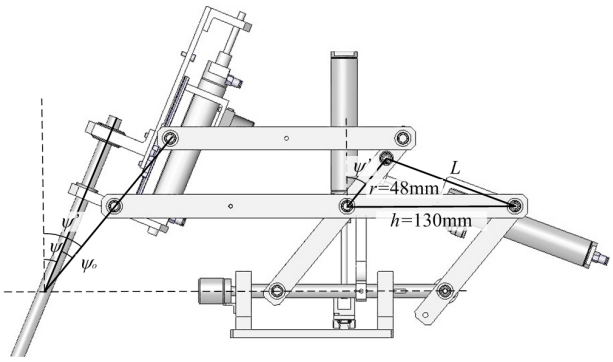

Fig. 3. Slider-Crank Mechanism

III. MASTER MANIPULATOR

The master manipulator for a surgical master-slave system is considered to have following features.

- wide moving range
- compact
- remain at the same position even the operator released their hands

For the translational movements of haptic interfaces, a delta mechanism are used well[10] because the mechanism can generate high power and keep the grip orientation constant during translational movements. We also adopted a delta mechanism for translation. In order to realize wide range of the orientation, we mounted a serial gimbal mechanism whose three rotational axes intersect at one point. Fig. 5 shows the developed master manipulator.

In this manipulator, AC servo motors with Harmonic Drive reduction gears are used as actuators. We used the

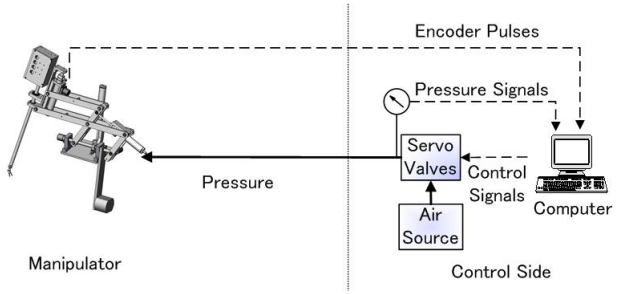

Fig. 4. System configuration

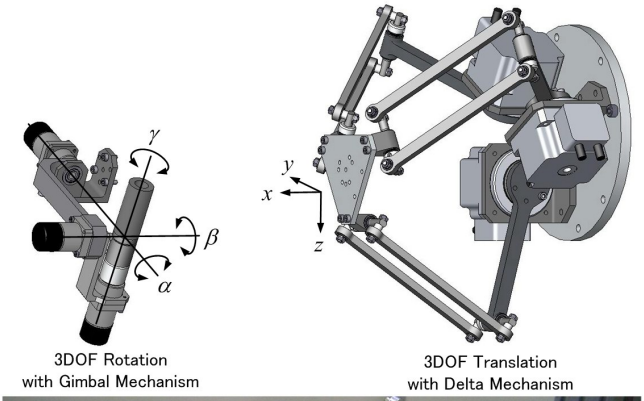

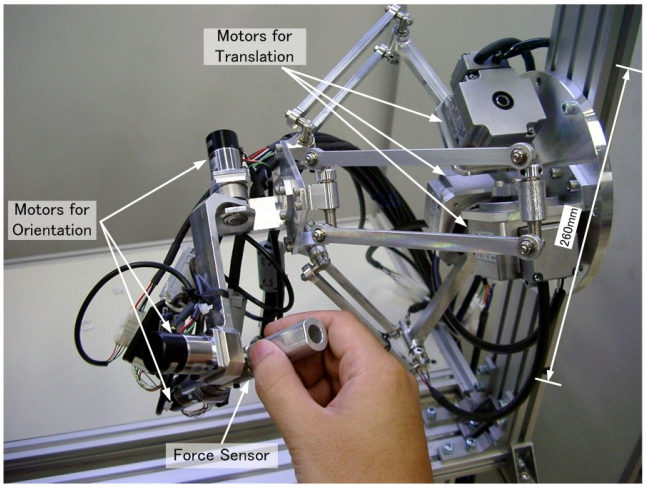

Fig. 5. Developed master manipulator

motors whose power is 40W (Harmonic Drive Systems Inc., FHA-8C-50-E200-CK) for translation and 20W (Harmonic Drive Systems Inc., RSF-5A-50-050-C) for orientation. The reduction ratio of the both actuators is 50. A 6-axes force sensor (BL AUTOTEC.LTD.,NANO2.5/2) is installed near the end-effector to measure the force exerted by operator. The measuring point of the force is corresponds to the center of rotation so that the amount of calculation can be reduced. The specification of the manipulator is shown in Table II.

IV. Master Slave Control

The goal of the control in master-slave system is to realize high transparency and provide good maneuverability that the operators feel as if doing some tasks with their own hands [11][12]. For this purpose, it may be required

TABLE II
SPECIFICATION OF THE MASTER MANIPULATOR

Force / Torque	50 N / 0.9 Nm
Translational Working Range	cubic whose diameter is 160mm
Rotational Working Range	$\alpha : \pm 160$, $\beta : \pm 80$, $\gamma : \pm 180$
DOF	6

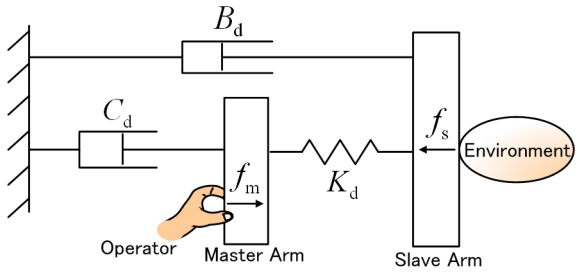

Fig. 6. Equivalent model of the impedance-controlled master-slave system

that both the position response and the force response are identical, whatever the object dynamics is. However, the safe operation is depended totally to the operator with this concept. The unexpected movement including shake of the operator's hands will transmitted to the slave side.

Therefore, we consider a compliance control of the slave manipulator using the compressibility of air effectively in order to avoid a large load to the organs of a patient. In this case, a contact between the slave manipulator and a external environment yield a deviation due to the compliance. As a surgeon is watching the slave side with a endoscope during the operation, maneuverability will be secured even there are some difference in position between the master and the slave side. On the other hand, the master arm with moderate damping effect can realize stable operation with preventing hand jiggling and too much speed.

We control the master and slave to have following impedance characteristics:

$$\text{slave}: \quad -\boldsymbol{f}_\mathrm{s} = K_\mathrm{d}(\boldsymbol{x}_\mathrm{s} - \boldsymbol{x}_\mathrm{m}) + B_\mathrm{d}\dot{\boldsymbol{x}}_\mathrm{s} \tag{8}$$

$$\text{master}: \quad \boldsymbol{f}_\mathrm{m} - \boldsymbol{f}_\mathrm{s} = C_\mathrm{d}\dot{\boldsymbol{x}}_\mathrm{m} \tag{9}$$

where

$\boldsymbol{x}_\mathrm{s}$	:	Slave position at Cartesian coordinate
$\boldsymbol{x}_\mathrm{m}$	:	Master position at Cartesian coordinate
$\boldsymbol{f}_\mathrm{s}$	:	Force applied to the object
$\boldsymbol{f}_\mathrm{m}$	:	Force applied to the master manipulator
K_d	:	Stiffness of the slave manipulator
B_d	:	Viscous coefficient the slave manipulator
C_d	:	Viscous coefficient the master manipulator

Here, we added B_d to improve the stability. The equivalent model of these characteristics is represented as shown in Fig. 6.

The impedance control is classified into force control type and motion (admittance) control type. For pneumatic manipulators, the impedance control based on force control is considered to be effective because of high back drivability and flexible characteristics. Therefore, a torque base impedance control without using force sensors [7] is applied.

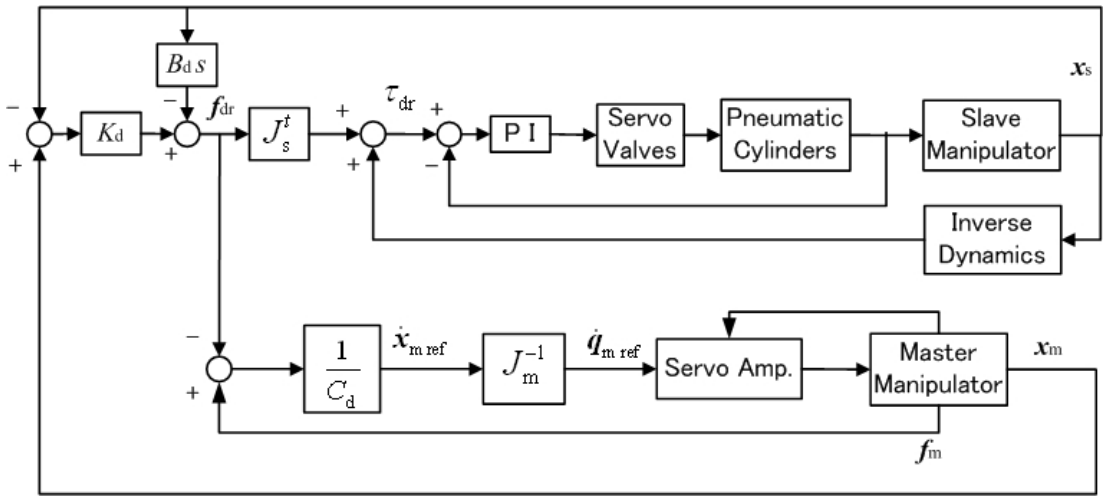

Fig. 7. Schematic block diagram of proposed bilateral control

The dynamic equations of the slave side in joint coordinate are given as follows;

$$\boldsymbol{\tau}_{\mathrm{dr}} - J_{\mathrm{s}}^{t}\boldsymbol{f}_{\mathrm{s}} = \boldsymbol{Z}(\boldsymbol{q}_{\mathrm{s}}, \dot{\boldsymbol{q}}_{\mathrm{s}}, \ddot{\boldsymbol{q}}_{\mathrm{s}}) \tag{10}$$

where

$\boldsymbol{\tau}_{\mathrm{dr}}$: driving torque by the actuator at each joint
$\boldsymbol{Z}$: inverse dynamics function of the manipulator
$\boldsymbol{q}$: displacement of each joint
J_{s} : Jacobian matrix of the slave manipulator

The driving torque to the actuators is given as

$$\boldsymbol{f}_{\mathrm{dr}} = K_{\mathrm{d}}(\boldsymbol{x}_{\mathrm{s}} - \boldsymbol{x}_{\mathrm{m}}) + B_{\mathrm{d}}\dot{\boldsymbol{x}}_{\mathrm{s}} \tag{11}$$

$$\boldsymbol{\tau}_{\mathrm{dr}} = -J_{\mathrm{s}}^{t}\boldsymbol{f}_{\mathrm{dr}} + \boldsymbol{Z}(\boldsymbol{q}_{\mathrm{s}}, \dot{\boldsymbol{q}}_{\mathrm{s}}, \ddot{\boldsymbol{q}}_{\mathrm{s}}). \tag{12}$$

Equation (8) could be derived by substituting (11) and (12) to (10) assuming that the dynamic response of the actuator is fast enough to provide the force. The calculated torque given by (12) is transformed to the driving force to the cylinder using (2) and (6) and is controlled using a PI controller. The bandwidth of the force control of the cylinder was achieved to be 40Hz despite time delays caused by air tubes with a length of about 1 meter.

Although, the accuracy of the force sensing will be worse compared with using force sensors attached to the tip part of the end effector, the force could be detective even the external force is given at any position of the manipulator. Therefore, the applied force which is blind from the endoscope could also be displayed to the operator. This will contribute to the safe operation.

On the other hand, the dynamics of the master manipulator has a high bandwidth with using a reduction gear with AC motors. As a result, an admittance control is suitable, because the dynamics of the manipulator and the effect of the gravity could be compensated and also it is easy to remain the position when the operator released one's hand. Therefore, we applied an admittance control expressed as

$$\dot{\boldsymbol{x}}_{\mathrm{m}} = (\boldsymbol{f}_{\mathrm{m}} - \boldsymbol{f}_{\mathrm{s}}) / C_{\mathrm{d}} \tag{13}$$

$$\dot{\boldsymbol{q}}_{\mathrm{m}} = J_{\mathrm{m}}^{-1}\dot{\boldsymbol{x}}_{\mathrm{m}}. \tag{14}$$

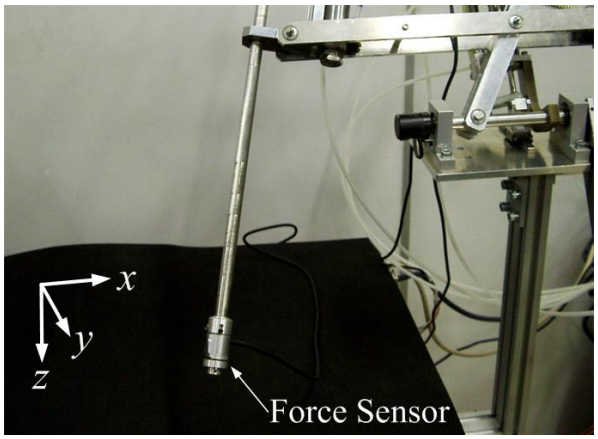

Fig. 8. Mounted force sensor for evaluation

On the control at the master side, the force applied to the slave manipulator from the object $\boldsymbol{f}_{\mathrm{s}}$ must be needed as described in (9). However, if the impedance control is successfully realized as shown in (8), $\boldsymbol{f}_{\mathrm{dr}}$ becomes equal to $\boldsymbol{f}_{\mathrm{s}}$. Therefore, $\boldsymbol{f}_{\mathrm{dr}}$ could be used for the estimated value of $\boldsymbol{f}_{\mathrm{s}}$. As a result, the controller can be summarized in a block diagram as shown in Fig. 7.

V. Experimental Results

A. Impedance control of the slave manipulator

The impedance control was applied to the developed slave manipulator to confirmed the controllability. A 6-DOF force sensor (BL AUTOTEC.LTD., NANO2.5/2) was attached to the tip of the forceps which was substituted with a pipe at this experiment as shown in Fig. 8. The measured force with the force sensor and the estimated force from the proposed method was compared. The impedances and the control gains used in the experiments were as follows:

K_{d} 0.2 N/mm
B_{d} 0.01 Ns/mm .

$\boldsymbol{Z}$ in (12) was identified from the data with some no contact motion. Fig. 9 shows the experimental results when the external force was applied at the tip of forceps during circular

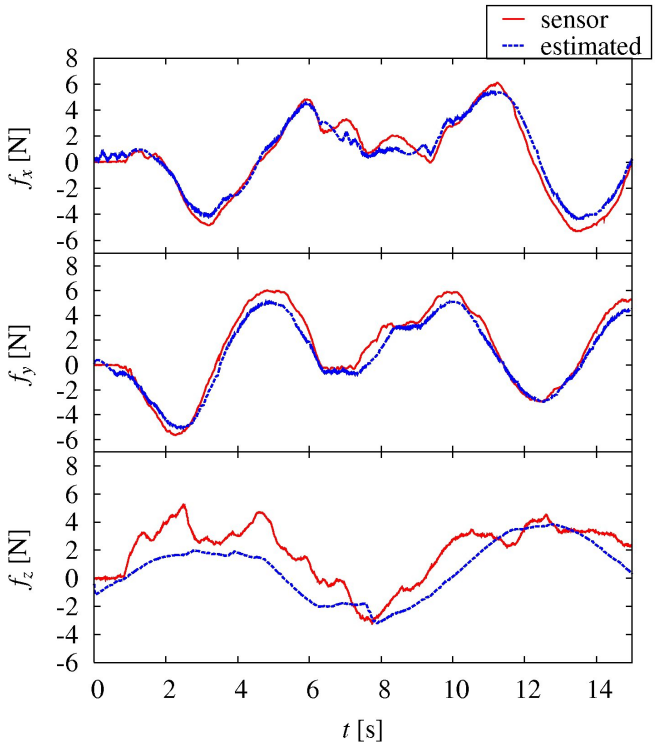

Fig. 9. Experimental results of force estimation

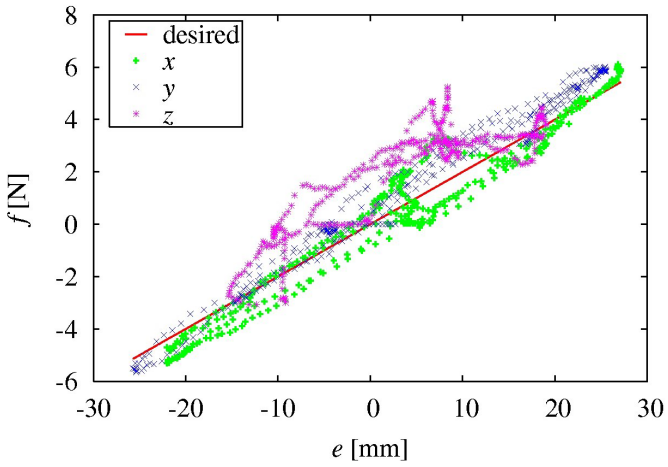

Fig. 10. Experimental results of the compliance control

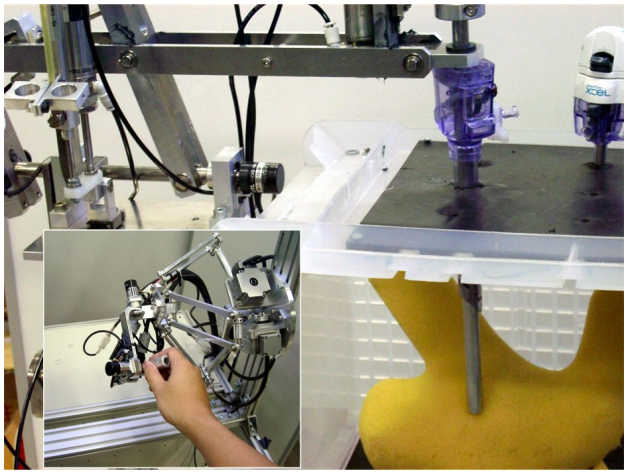

Fig. 11. Experiment of master-slave system

motion. In Fig. 9, the lateral axis shows the time and the longitudinal axis shows the applied force. The red lines indicate the results estimated by the proposed method $\boldsymbol{f}_{\mathrm{dr}}$ and the blue lines the measured values $\boldsymbol{f}_{\mathrm{s}}$. It is obvious from Fig. 9 that the force is well estimated at x and y direction. However, the force at z direction has some error. This is because of the friction force to the linear guide, which supports the z direction motion, becomes larger as the applied force to the y direction becomes larger. This could be solved by replacing the linear guide which will be strong to the radial stress.

Fig. 10 shows the experimental results of compliance control where the lateral axis shows positioning deviation between master and slave $\boldsymbol{e} = \boldsymbol{x}_{\mathrm{m}} - \boldsymbol{x}_{\mathrm{s}}$ and the longitudinal axis shows the stiffness term of the contact force $\boldsymbol{f} \equiv \boldsymbol{f}_{\mathrm{s}} - B_{\mathrm{d}}\dot{\boldsymbol{x}}$. While the error along z axis are, as mentioned above, relatively large compared with other axes and the maximum error is 3N, it can be seen that the isotropic compliance is realized.

B. Master-Slave Control

Next, the master-slave system was operated with the impedance control setting the damping ratio C_{d} at 0.006[Ns/mm]. Fig. 11 shows the experimental appearance. In this experiment, 3-DOFs for the wrist movement at the master side was stabled. Also a threshold was given to the estimated force to make the system stable. The configuration of the master-slave system for the experiment is presented in Fig. 12.

Fig. 13 shows the experimental results of the position and the force of y direction when the slave was moved with no contact to the object. It can be seen that the motion of the slave followed well with that of the master. The operating force applied to the master arm is proportional to the speed of the manipulator. While we gave the low viscous coefficient in this experiment, the operator could feel the light manipulability.

Fig. 14 shows the experimental results when the slave arm was brought into contact with a sponge object as shown Fig. 11. The operator stepwise increased and decreased the magnitude of the force during the experiment. It can been seen that the deviation of the slave position from the master trajectory is proportional to the force and the forces of the master and the slave are in good agreement. Therefore, the desired compliance characteristics was realized and the operator could sense the force at the slave side.

We will improve the performance of the impedance control and the force estimation. We will also equip the manipulator with the forceps manipulator and evaluate the maneuverability changing the impedance and scaling factor.

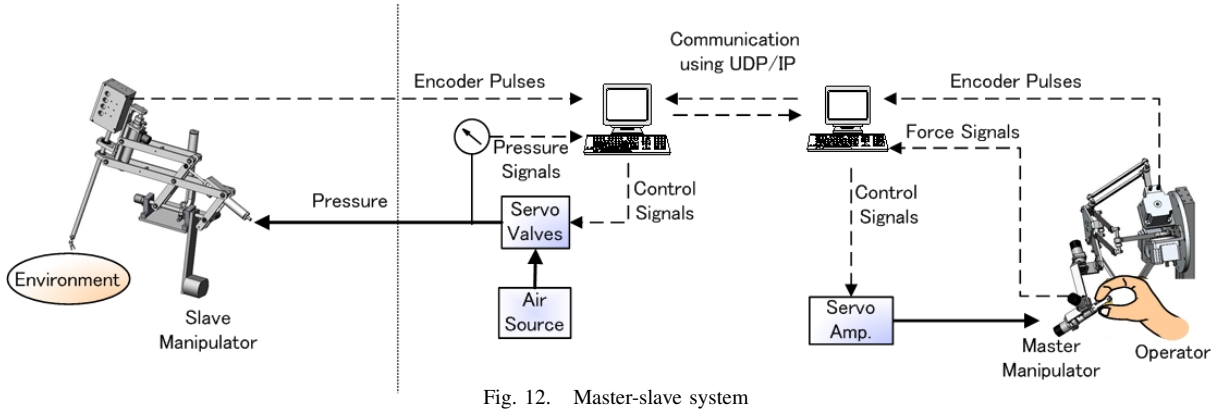

Fig. 12. Master-slave system

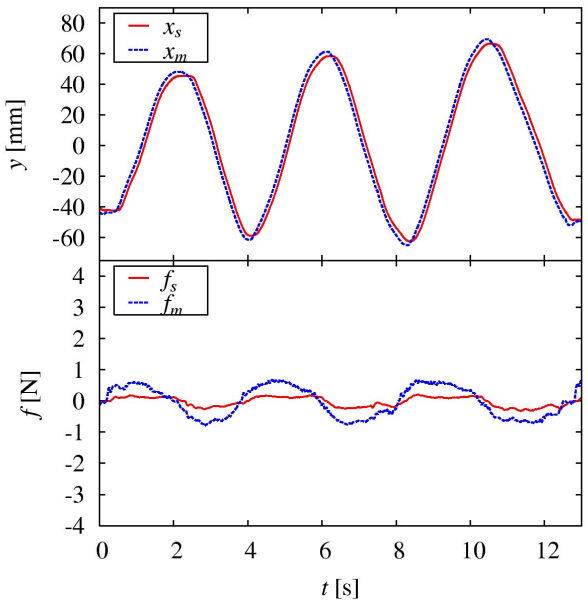

Fig. 13. Experimental results of bilateral control without contact

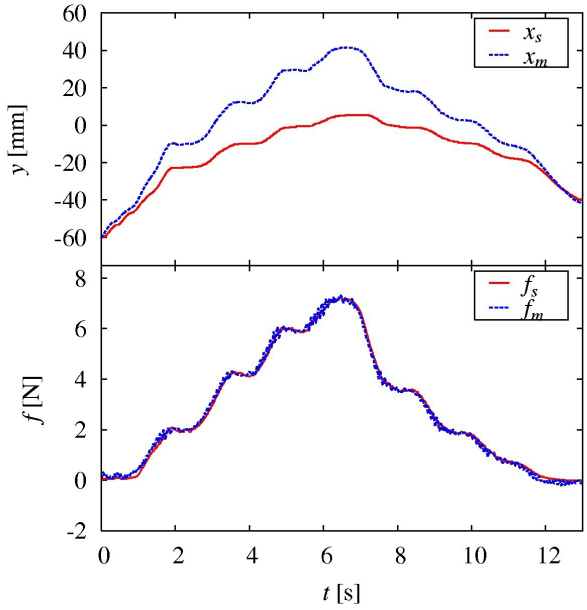

Fig. 14. Experimental results of bilateral control with contact

VI. Conclusion

In this paper, a manipulator for supporting forceps was developed which has 3-DOFs actuated by pneumatic cylinders. And we also developed a master manipulator using a delta mechanism and a gimbal mechanism with a force sensor and motors with Harmonic Drive. In the developed master-slave system, we applied different impedance control to each manipulator. For the pneumatic slave manipulator, we adopted the force control type of the impedance control without force sensor. The master manipulator with geared motors was implemented the admittance control. The experimental results indicated that the operator felt the force at the slave side with uncertainty of about 3N.

References

[1] Russell H. Taylor and Dan Stioianovici, Medical Robotics in Computer-Integrated Surgery, IEEE Trans. on Robotics and Automation, Vol.19, No.5, 2003, pp.765-780

[2] Davies, B.L., A review of Robotics in Surgery, Journal of Engineering in Medicine, Vol.213, 2000

[3] M. Hashizume et al., Early experience of endoscopic procedures in general surgery assisted by a computer-enhanced surgical system, Surgical Endoscopy, Vol.16, 2002, pp.1187-1191

[4] Hubens G. et al., A performance study comparing manual and robotically assisted laparoscopic surgery using the da Vinci system, Surgical Endoscopy, Vol.17, 2003, pp.1595-1599

[5] Gerovichev O, Marayong P, Okamura AM, The Effect of Visual and Haptic Feedback on Computer-Assisted Needle Insertion, Computer-Aided Surgery, Vol.9, No.6, pp.243-249, 2004.

[6] J. T. Dennerlein, D. B. Martin and H. Zak, Haptic Force-Feedback Devices for the Office Computer: Performance and Musculoskeletal Loading Issues, Human Factors, vol.43, No.2, pp.278-286, 1996

[7] S. Tachi, T. Sakaki, H. Arai, S. Nishizawa and Jose F. Pelaez-Polo, Impedance Control of a Direct-drive Manipulator without Using Force Sensors, Advanced Robotics, Vol. 5, No. 2, pp.183-205 (1991)

[8] A. J. Madhani, G. Niemeyer, and J. K. Salisbury, The Black Falcon: A Teleoperated Surgical Instrument for Minimally Invasive Surgery, IEEE/RSJ International Conference on Intelligent Robotic Systems, Vol.2, pp.936-944, 1998

[9] K. Tadano and K. Kawashima, Development of 4-DOFs Forceps with Force Sensing using Pneumatic Servo System, Proc. of IEEE/ICRA, pp.2250-2256 (2006)

[10] Tsumaki, Y., Naruse, H., Nenchev, D. N., Uchiyama, M., Design of a Compact 6-DOF Haptic Interface, Proceedings of the 1998 IEEE ICRA, Leuven, Belgium, May 1998.

[11] Yokokohji Y. and Yoshikawa Y., Bilateral Control of Master-Slave Manipulators for Ideal Kinesthetic Coupling, IEEE Trans. on Robotics and Automation, Vol.10, No.5, 1994,pp605-620

[12] Hannaford B., Design framework for teleoperations with kinematic feedback, IEEE Tanas, on Robotics and Automation, Vol.5, pp.426-434, 1998